Article

Cell Reports

FXR1P Limits Long-Term Memory, Long-Lasting Synaptic Potentiation, and De Novo GluA2 Translation

Graphical Abstract

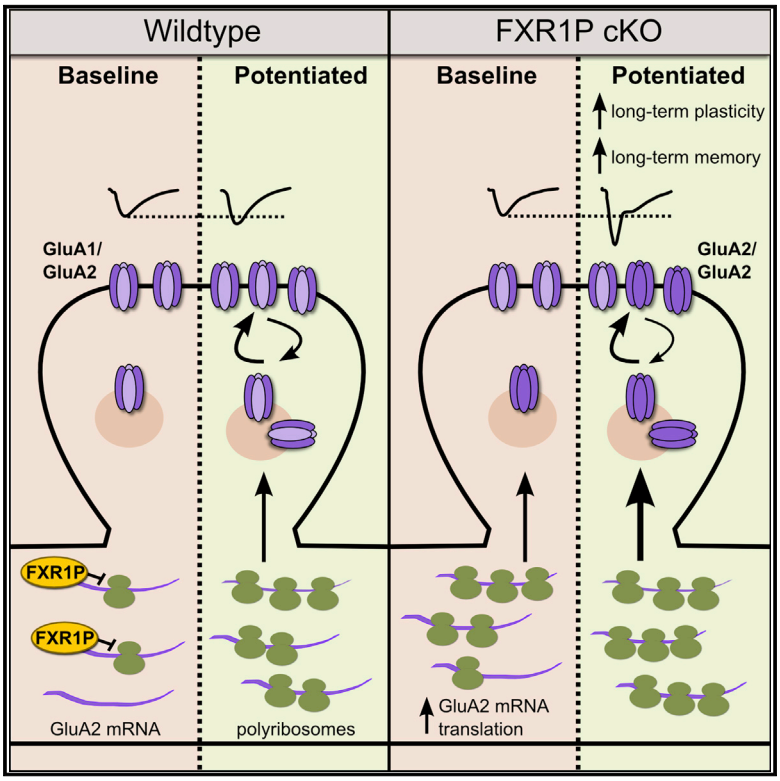

Highlights

Removal of FXR1P increases protein synthesis-dependent L-LTP and memory storage

FXR1P limits GluA2 synthesis and its activity-dependent synaptic delivery

FXR1P represses GluA2 mRNA translation via a GU-rich element in its 5′ UTR

Fragile X proteins have divergent roles in synaptic plasticity and memory storage

Authors

Denise Cook, Erin Nuro, ..., Jean-Claude Béïque, Keith K. Murai

Correspondence

keith.murai@mcgill.ca

In Brief

Control over protein synthesis is important for long-lasting plasticity and memory storage in the brain. Cook, Nuro, et al. now reveal that the RNA-binding protein FXR1P acts as a molecular brake that limits synthesis and synaptic incorporation of the AMPAR subunit GluA2, ultimately constraining long-term plasticity and memory formation.

Cook et al., 2014, Cell Reports 9, 1402–1416
November 20, 2014 ©2014 The Authors
http://dx.doi.org/10.1016/j.celrep.2014.10.028

OPEN ACCESS
CellPress

Cell Reports
Article

FXR1P Limits Long-Term Memory, Long-Lasting Synaptic Potentiation, and De Novo GluA2 Translation

Denise Cook,[1,7] Erin Nuro,[1,7] Emma V. Jones,[1] Haider F. Altimimi,[1] W. Todd Farmer,[1] Valentina Gandin,[2] Edith Hanna,[1] Ruiting Zong,[3] Alessandro Barbon,[4] David L. Nelson,[3] Ivan Topisirovic,[2] Joseph Rochford,[5] David Stellwagen,[1] Jean-Claude Béïque,[6] and Keith K. Murai[1,*]

[1]Centre for Research in Neuroscience, Department of Neurology and Neurosurgery, The Research Institute of the McGill University Health Centre, Montreal General Hospital, Montreal, QC H3G 1A4, Canada
[2]Lady Davis Institute for Medical Research, Sir Mortimer B. Davis Jewish General Hospital, and Department of Oncology, McGill University, Montreal, QC H3T 1E2, Canada
[3]Department of Molecular and Human Genetics, Baylor College of Medicine, Houston, TX 77030, USA
[4]Department of Molecular and Translational Medicine, National Institute of Neuroscience, University of Brescia, Brescia 25123, Italy
[5]Department of Psychiatry, Douglas Mental Health University Institute, McGill University, Verdun, QC H4H 1R3, Canada
[6]Department of Cellular and Molecular Medicine and Canadian Partnership for Stroke Recovery, University of Ottawa, Ottawa, ON K1H 8M5, Canada
[7]Co-first author
*Correspondence: keith.murai@mcgill.ca
http://dx.doi.org/10.1016/j.celrep.2014.10.028

SUMMARY

Translational control of mRNAs allows for rapid and selective changes in synaptic protein expression that are required for long-lasting plasticity and memory formation in the brain. Fragile X Related Protein 1 (FXR1P) is an RNA-binding protein that controls mRNA translation in nonneuronal cells and colocalizes with translational machinery in neurons. However, its neuronal mRNA targets and role in the brain are unknown. Here, we demonstrate that removal of FXR1P from the forebrain of postnatal mice selectively enhances long-term storage of spatial memories, hippocampal late-phase long-term potentiation (L-LTP), and de novo GluA2 synthesis. Furthermore, FXR1P binds specifically to the 5′ UTR of GluA2 mRNA to repress translation and limit the amount of GluA2 that is incorporated at potentiated synapses. This study uncovers a mechanism for regulating long-lasting synaptic plasticity and spatial memory formation and reveals an unexpected divergent role of FXR1P among Fragile X proteins in brain plasticity.

INTRODUCTION

Memories are thought to be stored as long-lasting changes in the size, strength, and number of synapses in neuronal networks (Govindarajan et al., 2006; Kessels and Malinow, 2009). These changes rely on new protein synthesis that occurs locally from translational machinery found in dendrites and at synapses (Schuman et al., 2006). This local protein synthesis is regulated through a combination of general translational control mechanisms, which act on all mRNAs, and gene-specific mechanisms, which act on specific subsets of mRNAs. Together, these mechanisms ensure that the correct proteins are synthesized in response to specific patterns of synaptic activity (Costa-Mattioli et al., 2009). Although several studies have shown that knocking out components of the general translational control pathway alters and even enhances synaptic plasticity and memory (Costa-Mattioli et al., 2005, 2007; Kelleher et al., 2004), further elucidation of the role of gene-specific mechanisms in these processes is required.

In the brain, gene-specific mRNA translational control is achieved by a diverse array of neuronal RNA-binding proteins whose roles in long-term plasticity and memory storage remain largely unexplored (Doyle and Kiebler, 2011; Elvira et al., 2006; Kanai et al., 2004). One of these RNA-binding proteins, Fragile X Related Protein 1 (FXR1P), is related to FXR2P and Fragile X Mental Retardation Protein (FMRP), two proteins that are known to function in synaptic plasticity and memory. Although it has been shown that FXR1P can regulate protein synthesis in nonneuronal cells (Garnon et al., 2005; Vasudevan and Steitz, 2007), its role in mRNA translation and synaptic plasticity in neurons is unknown, largely because complete loss of FXR1P in mice results in perinatal lethality (Mientjes et al., 2004). Our recent discovery that FXR1P colocalizes with translation machinery in dendrites and near a subset of dendritic spines (Cook et al., 2011) prompted us to investigate its function in brain development, plasticity, and synaptic protein expression, and to compare its role with those of FXR2P and FMRP.

To address the in vivo role of FXR1P in the brain, we conditionally deleted FXR1P from the postnatal forebrain of mice and found that loss of FXR1P specifically enhances hippocampal protein synthesis-dependent late-phase long-term

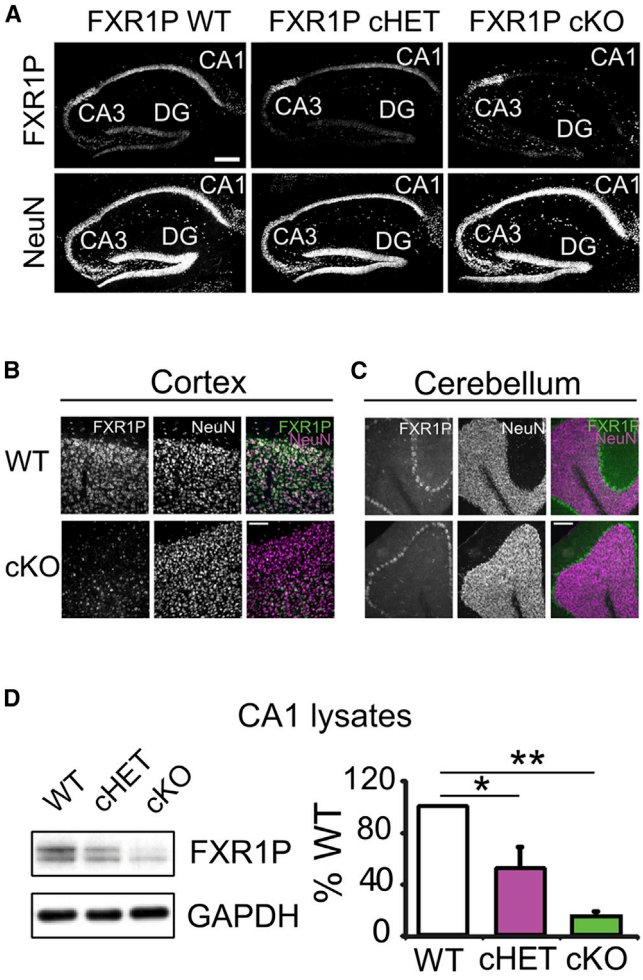

Figure 1. Characterization of FXR1P cKO Mice

(A) Hippocampal sections taken from postnatal day 60 WT, cHET, and cKO mice labeled for FXR1P and NeuN. FXR1P is lost from CA1 cells in cHET and cKO mice (n = 3 mice/genotype). Scale bar, 200 μm.

(B and C) FXR1P is lost from cortical neurons (B), but not cerebellar Purkinje cells (C). Scale bar, 100 μm.

(D) Western blots of CA1 lysates from WT, cHET, and cKO mice. FXR1P is reduced in the cHET and cKO mice (one-way ANOVA, $F_{(2, 6)} = 16.66$, $p = 0.004$, Tukey HSD post hoc, $p < 0.05$; n = 3 mice/genotype from 3 litters). Error bars show SE. $^{**}p \leq 0.01$, $^{*}p \leq 0.05$.

See also Figure S1.

potentiation (L-LTP), spatial memory, and expression of the AMPA receptor subunit GluA2. Furthermore, we show that FXR1P binds to GluA2 mRNA and represses its translation through a conserved GU-rich element in its 5′ UTR. Interestingly, the ability of FXR1P to repress GluA2 synthesis is unique to FXR1P and is not a property of FXR2P or FMRP. Ultimately, the loss of FXR1P-mediated GluA2 repression heightens activity-dependent synaptic delivery of GluA2, increasing its incorporation at potentiated synapses. Thus, FXR1P has a critical role in limiting synaptic plasticity and memory storage in the brain, and serves an unexpected divergent function among Fragile X proteins in these processes.

RESULTS

Characterization of FXR1P Conditional Knockout Mice

To investigate the role of FXR1P in the brain, we genetically removed FXR1P from excitatory neurons in the forebrain of early postnatal mice using a floxed *Fxr1* line combined with the αCaMKII-Cre T29-1 transgenic line (Sonner et al., 2005; Tsien et al., 1996). Using a fluorescent reporter line, we found that Cre-mediated recombination in CA1 cells started around postnatal day 12 and was nearly complete by postnatal day 60 (Figure S1A). Recombination was not seen in cerebellar and midbrain regions, as previously reported (Sonner et al., 2005).

To verify Cre-mediated loss of FXR1P from CA1 cells, we labeled hippocampal sections from adult wild-type (WT), FXR1P conditional heterozygous (cHET), and FXR1P conditional knockout (cKO) mice with FXR1P and NeuN antibodies. This revealed that FXR1P was lost from the majority of CA1 cells (Figure 1A). As expected, FXR1P was eliminated from many neurons in the cortex but was maintained in cerebellar Purkinje cells (Figures 1B and 1C). Using protein lysates from area CA1, we found that FXR1P levels were reduced to 52% (cHET) and 15% (cKO) of WT levels (Figure 1D).

Analysis of cKO mice showed that hippocampal anatomy was unperturbed by the loss of FXR1P. This was shown by labeling for neurons (NeuN) (Figure 1A), dendrites (MAP2), ribosomes (P0), and astrocytes (GFAP) (Figure S1B). No changes in these markers were observed, indicating that loss of FXR1P did not change the overall cell morphology or organization. To determine whether synapse density and morphology were changed, we labeled CA1 cells with DiI and analyzed spine density, size, and shape in adult mice. This revealed that loss of FXR1P caused a 15% reduction in spine density and an 8% decrease in spine length without changing the head diameter or shape (Figures S1C–S1G). Thus, loss of FXR1P reduces spine density and length.

FXR1P cKO Mice Show Enhanced Long-Term Memory Storage

To determine whether loss of FXR1P alters behavior, we tested cKO mice on paradigms that assess basic motor/sensory function, anxiety, learning, and memory. cKO mice showed no deficits in motor/sensory function or anxiety, as tested using the open-field test and light/dark box (Figures S2A and S2B). Both genotypes also performed equally well on strong and weak contextual fear conditioning paradigms (Figure S2C; not shown) and on the object recognition test (a test of working memory) (Figure S2D). These results suggest that basic motor/sensory function, anxiety, contextual fear memory, and working memory are intact in cKO mice.

To test for a more specific role of FXR1P in spatial learning/memory, we used a modified Morris water maze paradigm that assesses learning, long-term memory storage, and behavioral flexibility (Figure 2A). WT and cKO mice performed equally well during the initial 5 training days (Figure 2A). However, during a probe trial conducted 4 hr after the last training session, the cKO mice spent more time in the target quadrant and crossed the target platform location more often than the WT mice, suggesting that they had acquired a better spatial memory of

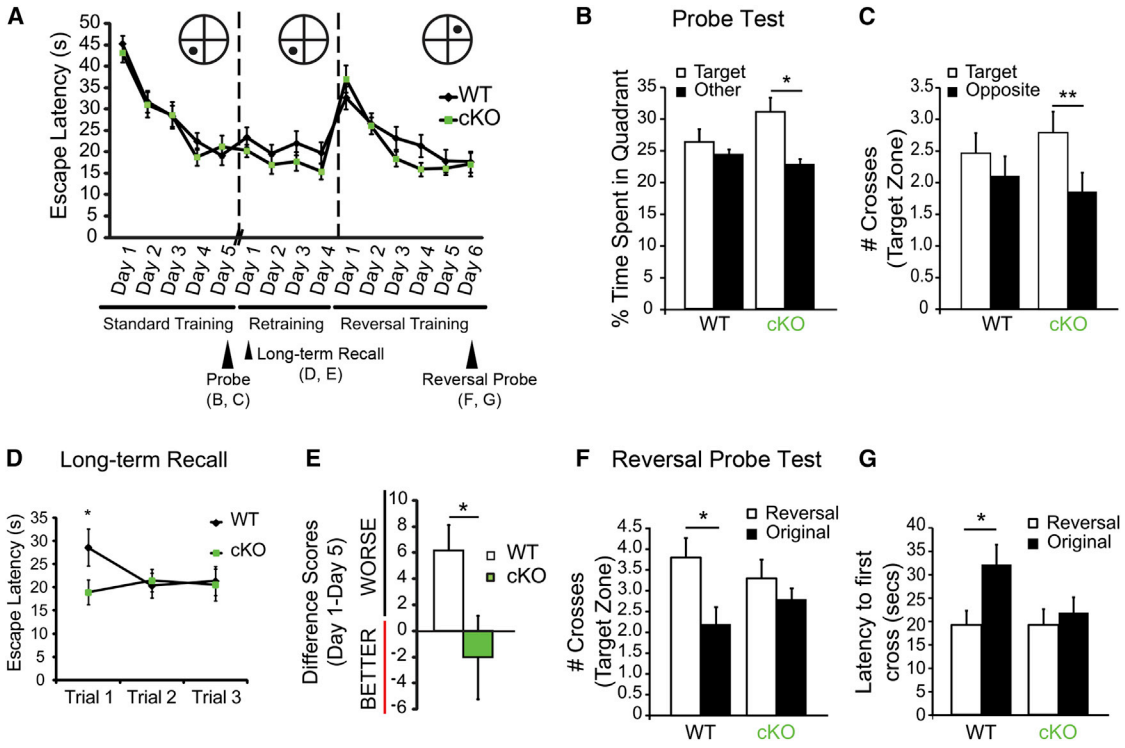

Figure 2. Loss of FXR1P Enhances Long-Term Memory and Behavioral Flexibility

(A) cKO mice perform similarly to WT mice in the learning trials of Morris water maze training (two-way mixed ANOVA [genotype, days], main effect days, $F_{(4, 208)} = 46.52$, $p < 0.001$), retraining (two-way mixed ANOVA [genotype, days], $p > 0.05$), and reversal training (two-way mixed ANOVA [genotype, days], main effect days, $F_{(5, 180)} = 24.73$, $p < 0.001$).

(B and C) cKO mice perform better than WT mice on the probe test 4 hr after the third trial on training day 5.

(B) cKO mice spend more time in the target quadrant compared with the average of all other quadrants (two-tailed paired t test, $t(27) = 2.73$, $p = 0.01$), whereas WT mice do not (two-tailed paired t test, $t(27) = 0.6784$, $p = 0.50$).

(C) cKO mice cross the platform in the target zone more frequently than the platform in the opposite zone (two-tailed paired t test, $t(27) = 2.79$, $p = 0.01$), whereas WT mice do not (two-tailed paired t test, $t(27) = 0.79$, $p = 0.44$).

(D and E) cKO mice have enhanced ability to recall long-term memories 9 days after the original 5 training days.

(D) cKO mice are faster at locating the hidden platform on the first trial of the first day of retraining (two-tailed unpaired t test, $t(33) = 2.01$, $p = 0.05$).

(E) cKO mice perform equally well on the first day of retraining (average of three trials) compared with their performance on the last day of the original learning phase (average of three trials), whereas WT mice are slower (two-tailed unpaired t test, $t(31) = 2.19$, $p = 0.04$).

(F and G) cKO mice do not show a preference for the new platform location in the reversal probe test.

(F) WT mice cross the new platform location more often than the old platform location during the probe test (two-tailed paired t test, $t(19) = 2.49$, $p = 0.02$), whereas cKO mice do not (two-tailed paired t test, $t(19) = 0.92$, $p = 0.37$).

(G) WT mice display a shorter latency to first cross for the new platform location versus the old platform location (two-tailed paired t test, $t(19) = 2.40$, $p = 0.03$), whereas cKO mice show an equivalent latency to first cross of the reversal and original platform locations (two-tailed paired t test, $t(19) = 0.57$, $p = 0.57$).

Error bars show SE. *$p \leq 0.05$, **$p \leq 0.01$. See also Figure S2.

the platform location as compared with WT mice (Figures 2B and 2C).

Consistent with the improved performance of cKO mice in the probe test, when the mice were retested 9 days later, cKO mice were faster than WT mice at locating the platform. This improved recall was demonstrated both by a reduction in escape latency during the first trial of retraining (day 1; Figure 2D) and by differences in the average performance of the mice on day 1 of retraining versus day 5 of the original training (Figure 2E). Thus, cKO mice showed an enhanced ability to recall spatial memories.

Since disruption of general protein synthesis can alter behavioral flexibility in spatial memory tasks (Hoeffer et al., 2008), we tested whether cKO mice can learn and remember a new platform location. Mice from both genotypes similarly learned the location of the new platform (Figure 2A). However, unlike WT mice, cKO mice failed to shift their preference to the new platform location during the reversal probe test (Figure 2F). Measuring the average latency to the first platform crossing further revealed that cKO mice showed an equal latency to first crossing of the original and reversal platform locations, unlike WT mice that immediately targeted the location of the reversal platform (Figure 2G). Interestingly, in contrast to other mouse mutants with disruptions in mRNA translation machinery, cKO mice did not display perseverative behavior during the learning phases or probe test (Hoeffer et al., 2008; Trinh et al., 2012), but in fact showed equal preferences for the original and reversal

platform locations. Together, these results indicate that FXR1P cKO mice have enhanced spatial memory without perseverative behaviors.

FXR1P cKO Mice Display a Specific Enhancement in L-LTP

Alterations in spatial memory are associated with changes in the function and plasticity of excitatory synapses in hippocampal area CA1. To determine whether cKO mice have altered synaptic function and plasticity that may affect learning and memory processes, we conducted a series of electrophysiology experiments. We recorded field potentials in the stratum radiatum and found no differences in the input-output relationship or paired-pulse ratio (a measure of presynaptic release probability; Dobrunz and Stevens, 1997) between genotypes (Figures 3A and 3B), indicating that cKO mice have normal basal synaptic strength and short-term plasticity, respectively.

We next tested cKO slices for their ability to establish and maintain both protein-synthesis independent (early-phase LTP [E-LTP]) and protein synthesis-dependent forms of synaptic plasticity (L-LTP, mGluR-LTD) (Kelleher et al., 2004). We induced E-LTP in WT and cKO slices using a single train of high-frequency stimulation (HFS; 1 × 100 Hz). We found that E-LTP was similar in both genotypes (Figure 3C). However, when we induced L-LTP by delivering four trains of HFS separated by a 20 s interval (4 × 100 Hz) (Scharf et al., 2002), we found that L-LTP was increased at both 20–30 min and 3 hr post-HFS in the cKO (Figures 3D and 3E). To test whether the loss of FXR1P has a general effect on protein synthesis-dependent long-term plasticity, we tested for DHPG-induced mGluR-LTD (Huber et al., 2002). However, cKO mice showed normal mGluR-LTD (Figure 3F). Thus, loss of FXR1P specifically enhanced L-LTP, a form of plasticity that depends on new protein synthesis, without perturbing E-LTP or mGluR-dependent LTD.

Increased Translation of GluA2 in FXR1P cKO Mice

Since FXR1P is detected in polyribosome fractions in mouse brain and localized with translation machinery at or near spines in neurons (Cook et al., 2011; Figure S3), we screened for changes in expression of molecules involved in protein translation and synaptic development/function in cKO mice. Importantly, probing hippocampal lysates showed that loss of FXR1P did not affect the levels of its paralogs, FMRP and FXR2P (Figure 4A). Consistent with immunolabeling for ribosomal protein P0 (Figure S1B), we also did not see changes in expression of eIF4E, a cap-binding subunit of the eIF4F complex that recruits mRNA to the ribosome (Hershey et al., 2012), or Argonaute 2 (AGO2), a component of the RNA-induced silencing complex (RISC). Neither Talin 2 nor desmoplakin, which are known to be altered in cardiac tissue of full FXR1P KO mice, were changed (Figure S4; Whitman et al., 2011). Blotting for vGlut1, PSD95, αCaMKII, and PKMzeta showed that levels of these synaptic proteins were also unaltered in cKO mice (Figure 4A).

Intriguingly, loss of FXR1P resulted in a significant increase in expression of the AMPAR subunit GluA2. This increase was specific for GluA2, as no changes in the levels of GluA1, GluA3, or the NMDAR subunit GluN1 were found (Figure 4A). To determine whether the FXR1P paralogs FXR2P and FMRP regulate GluA2 in a similar manner, we probed hippocampal lysates from FXR2P and FMRP KO mice. Unexpectedly, we observed a decrease in GluA2 in FXR2P KO mice that was not due to a compensatory change in FXR1P expression (Figure 4B). No alterations in GluA2 or FXR1P were detected in hippocampal lysates from FMRP KO mice (Figure 4B). These findings show that FXR1P reduces expression of GluA2 and indicate an intriguing divergence in the regulation of GluA2 by Fragile X-related proteins.

To determine whether GluA2 upregulation in FXR1P cKO mice was due to a change in transcription/stability of GluA2 mRNA, we quantified GluA2 mRNA (*Gria2*) levels using real-time quantitative RT-PCR (qRT-PCR). As expected, *Fxr1* mRNA levels were reduced by 50% in the hippocampus of cKO mice, but not the cerebellum, whereas equivalent levels of *Gria2* (GluA2) and *Grin1* (GluN1) mRNAs were found in cKO and WT mice (Figure 4C). This suggests that the elevation in GluA2 protein expression was not due to an increase in GluA2 mRNA transcription or stability.

To investigate whether the increase in GluA2 in cKO mice was due to increased mRNA translation, we used the surface sensing of translation (SUnSET) method (Schmidt et al., 2009). This method quantifies newly synthesized proteins by tagging them with puromycin. When we quantified total puromycin incorporation over a period of 45 min, we found no significant difference in global protein synthesis between genotypes (Figure 4D). However, immunoprecipitation (IP) of GluA2 and blotting for puromycin demonstrated a 59% increase in newly synthesized GluA2 in cKO mice (Figure 4E). This increase in GluA2 translation in cKO mice without a concomitant change in GluA2 mRNA abundance indicates that FXR1P represses (directly or indirectly) the translation of GluA2 mRNA in the brain.

FXR1P Represses mRNA Translation through a GU-Rich Element in the GluA2 5′ UTR

The long isoforms of GluA2 mRNA, which account for at least half of the GluA2 transcripts across various regions of the rat brain, are translationally repressed by elements within their 5′ UTR and 3′ UTR (Irier et al., 2009). However, the molecular events that control this repression are unknown. To test whether FXR1P is a mediator of GluA2 repression, we overexpressed FXR1P with eGFP reporter constructs containing either the 5′ or 3′ UTR of GluA2 in 293T cells and monitored eGFP protein levels (La Via et al., 2013; Figure 5A). Although FXR1P had no effect on eGFP expression from a control construct (Figure 5B), it significantly reduced expression of eGFP when the construct contained the 5′ UTR, but not the 3′ UTR, of GluA2 (Figure 5C). qRT-PCR experiments showed that FXR1P did not affect the levels of mRNAs from 5′ UTR and 3′ UTR eGFP constructs (Figure S5), indicating that FXR1P specifically regulates translation of the GluA2 5′ UTR reporter.

Myers et al. (2004) identified a GU-rich sequence within the 5′ UTR of long isoforms of GluA2 mRNA that they termed the "translation suppression domain." This sequence is predicted

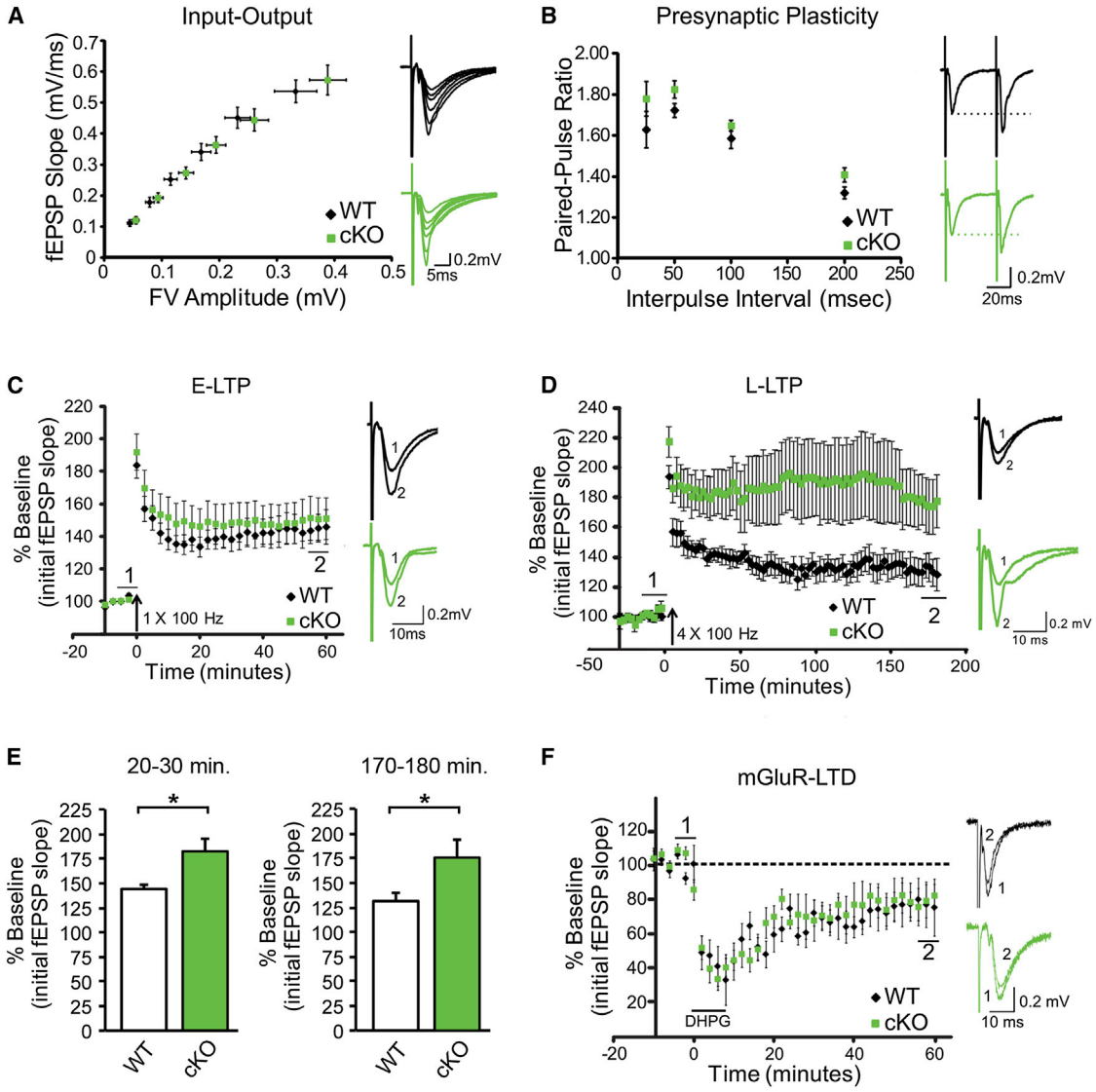

Figure 3. FXR1P cKO Mice Show a Specific Enhancement in L-LTP

(A) Left: input-output curve showing synaptic responses upon increasing stimulation intensities for WT and cKO mice. Right: representative traces from WT and cKO mice.

(B) Left: paired-pulse facilitation (PPF) is normal in cKO mice (two-way mixed ANOVA, genotype × interstimulus interval, $F_{(3,39)} = 0.44$, $p = 0.73$). Right: representative traces at a 50 ms interval.

(C) Left: E-LTP induced by a single train of HFS (1 × 100 Hz) is normal in cKO mice (n = 8 mice, 9 slices, from 4 litters; analysis at 50–60 min post-HFS, two-tailed unpaired t test, $t(15) = -0.38$, $p = 0.71$). Right: traces representing (1) 5 min of baseline immediately preceding HFS and (2) the period from 55–60 min post-LTP.

(D) Left: four trains of HFS delivered at 20 s intervals (HFS: 4 × 100 Hz) produce higher levels of potentiation in cKO animals (n = 7 mice, 7 slices, from 5 litters) than WT animals. Right: traces representing (1) 5 min of baseline immediately preceding HFS and (2) the period from 175–180 min post-LTP.

(E) L-LTP, measured at 20–30 min and 170–180 min post-HFS, is greater in cKO (two-tailed unpaired t tests, $t(7) = 2.65$, $p = 0.03$ and $t(9) = 2.24$, $p = 0.05$, respectively).

(F) Left: mGluR-dependent LTD is unchanged in cKO mice (two-tailed, unpaired two-sample t test, $p = 0.86$). Right: traces representing (1) 5 min of baseline immediately preceding bath application of DHPG (100 μM, 7–8 min) and (2) the period from 55–60 min after DHPG administration. Error bars show SE. Traces show an average of approximately 5–10 sweeps.

to form a stem-loop structure that suppresses GluA2 translation initiation. To determine whether FXR1P uses this sequence to repress GluA2 translation, we deleted the GU-rich element from the 5′ UTR and repeated the experiments above. Remarkably, loss of the GU-rich element prevented FXR1P from both repressing translation (Figure 5D) and binding to the GluA2 5′ UTR (Figure 5E).

To understand whether repression of GluA2 translation is specific for FXR1P, we repeated the experiments with FXR2P and FMRP. Surprisingly, we found that FXR2P enhanced eGFP levels

when either the 5′ or 3′ UTR was present (Figure 5F), whereas FMRP did not alter translation of eGFP (Figure 5G). These results agree with the FXR2P and FMRP KO data presented in Figure 4, suggesting that FXR1P represses expression of GluA2, whereas FXR2P promotes it. Together, our results uncover a divergent role of FXR1P (compared with FXR2P and FMRP) in repressing GluA2 translation.

Basal Surface Levels of GluA2 in FXR1P cKO Mice Are Unchanged

GluA2 is a transmembrane receptor that has functional properties at the cell surface. We next determined whether the overall increase in GluA2 expression in cKO mice caused a change in its surface level by performing surface biotinylation assays in hippocampal slices. Remarkably, the steady-state cell-surface levels of GluA2 were similar between genotypes (Figure 6A), consistent with the unaltered AMPAR-mediated field potentials in cKO mice (Figure 3A). Together, these results indicate that cKO mice have normal basal surface levels of GluA2 and a potential increase in intracellular GluA2 receptor subunits.

Activity-Dependent GluA2 Synthesis Is Intact in FXR1P cKO Mice

To determine whether loss of FXR1P alters the activity-driven increases in GluA2 translation seen during protein synthesis-dependent synaptic plasticity (Nayak et al., 1998), we subjected slices from both genotypes to forskolin-induced chemical LTP (cLTP; +forskolin, low Mg^{2+}), which reliably induces long-lasting synaptic potentiation that occludes electrically evoked L-LTP (Huang and Kandel, 1994; Otmakhov et al., 2004). As expected from other LTP studies, phosphorylation of serine 845 (pS845) on GluA1, a PKA phosphorylation site that is known to promote GluA1 trafficking to perisynaptic and extrasynaptic sites (Lee et al., 2000; Man et al., 2007; Oh et al., 2006), was significantly enhanced in WT and cKO slices upon cLTP (Figure S6A). Interestingly, we found that pS845 levels were significantly elevated in cKO slices even under basal conditions (Figure S6A). We next applied the SUnSET method to test whether cLTP-driven expression of de novo GluA2 was altered in cKO mice. Consistent with the results in Figure 4E, cKO slices showed a basal increase in de novo GluA2 (Figure 6C). Despite this basal increase, we found that cLTP caused an increase in GluA2 synthesis in both WT and cKO slices, and post-cLTP de novo GluA2 levels were similar between the genotypes (Figure 6C). Control experiments showed that neither cLTP nor loss of FXR1P resulted in an unspecific change in protein synthesis as monitored by GAPDH production (Figure S6B). These results show that overall activity-dependent de novo GluA2 translation is not altered in cKO mice and is unlikely to account for the differences in L-LTP.

Loss of FXR1P Increases cLTP-Driven Synaptic Incorporation of De Novo GluA2

Despite increased steady-state GluA2 expression in the cKO mice, we failed to detect significant cLTP-induced differences between the genotypes that may enhance L-LTP in cKO mice. This may be due to the fact that the experiments did not discriminate between subcellular compartments in neurons. To address this issue, we developed a method to investigate GluA2 expression at synapses using synaptosomal preparations (Figure S7A) combined with cLTP, SUnSET labeling, and IP/coimmunoprecipitation (coIP) techniques on acute slices. Based on our L-LTP and biochemistry results, we hypothesized that cKO mice would show enhanced cLTP-driven delivery of GluA2 subunits to synapses during an early stabilization phase of LTP (<1 hr). Thus, we tagged de novo translated GluA2 subunits with puromycin to monitor the translocation efficiency of GluA2 subunits to synapses. We found that newly synthesized GluA2 showed similar baseline incorporation into synapses in WT and cKO mice within 45 min (Figure 6D). This result corresponds well with our data indicating equal amounts of surface GluA2 in both genotypes under basal conditions (Figure 6A). However, de novo synthesized GluA2 subunits showed enhanced synaptic incorporation in cKO slices within 45 min after cLTP (Figure 6D). Enhanced synaptic GluA2 was corroborated by an increase in surface GluA2 in cKO slices upon cLTP (Figure S7B). This increase was specific to GluA2, as delivery of de novo GluN1 remained similar between the genotypes (Figure 6E). Interestingly, we also found that in WT slices, FXR1P levels were significantly reduced from both crude and synaptic fractions 45 min after cLTP, suggesting that native FXR1P protein can be dynamically regulated in WT neurons by activity (Figures S7C and S7D). Altogether, these results indicate that FXR1P controls the amount of GluA2 subunits that are selectively mobilized to synapses upon long-lasting synaptic plasticity.

FXR1P Controls AMPAR Composition at Potentiated Synapses

GluA1 and GluA2 comprise the majority of AMPAR subunits at hippocampal synapses (~80%; Lu et al., 2009) and GluA2 synaptic incorporation is critical for L-LTP (Migues et al., 2010; Yao et al., 2008). Given the enhanced activity-dependent delivery of GluA2 to synapses in the absence of FXR1P, we investigated whether AMPAR composition was changed at synapses in cKO mice. For this purpose, we coimmunoprecipitated GluA2 and GluA1 subunits from synaptosomes (Kang et al., 2012). Under basal conditions, comparable amounts of GluA2- and GluA1-containing AMPARs were coprecipitated with GluA2 and GluA1, respectively. This suggests a similar AMPAR composition at baseline in both genotypes (Figures 7A and 7B). However, following cLTP, significantly more GluA2 subunits coprecipitated with GluA2 in the cKO as compared with the WT mice, indicating that loss of FXR1P bolsters GluA2-GluA2 association (Figure 7A). The inverse case was found for GluA1 in the cKO, where IP of GluA1 resulted in less GluA1-containing AMPA receptors (Figure 7B). These changes were specific for AMPARs, as GluN1-containing synaptic complexes were unaffected in cKO mice (Figure S7E). These results suggest that FXR1P favors an increase in GluA2 over GluA1 subunits at synapses in cKO mice following cLTP.

To further dissect the composition of AMPARs at synapses in cKO mice following cLTP, we determined the relative amount of GluA1 that coassociated with GluA2, and vice versa, by either GluA2 IP and blotting for GluA1 or GluA1 IP and blotting for GluA2. Both IP combinations showed reduced association of GluA1 with GluA2 at synapses of cKO slices following cLTP (Figures 7C and 7D). To discriminate whether this reduced

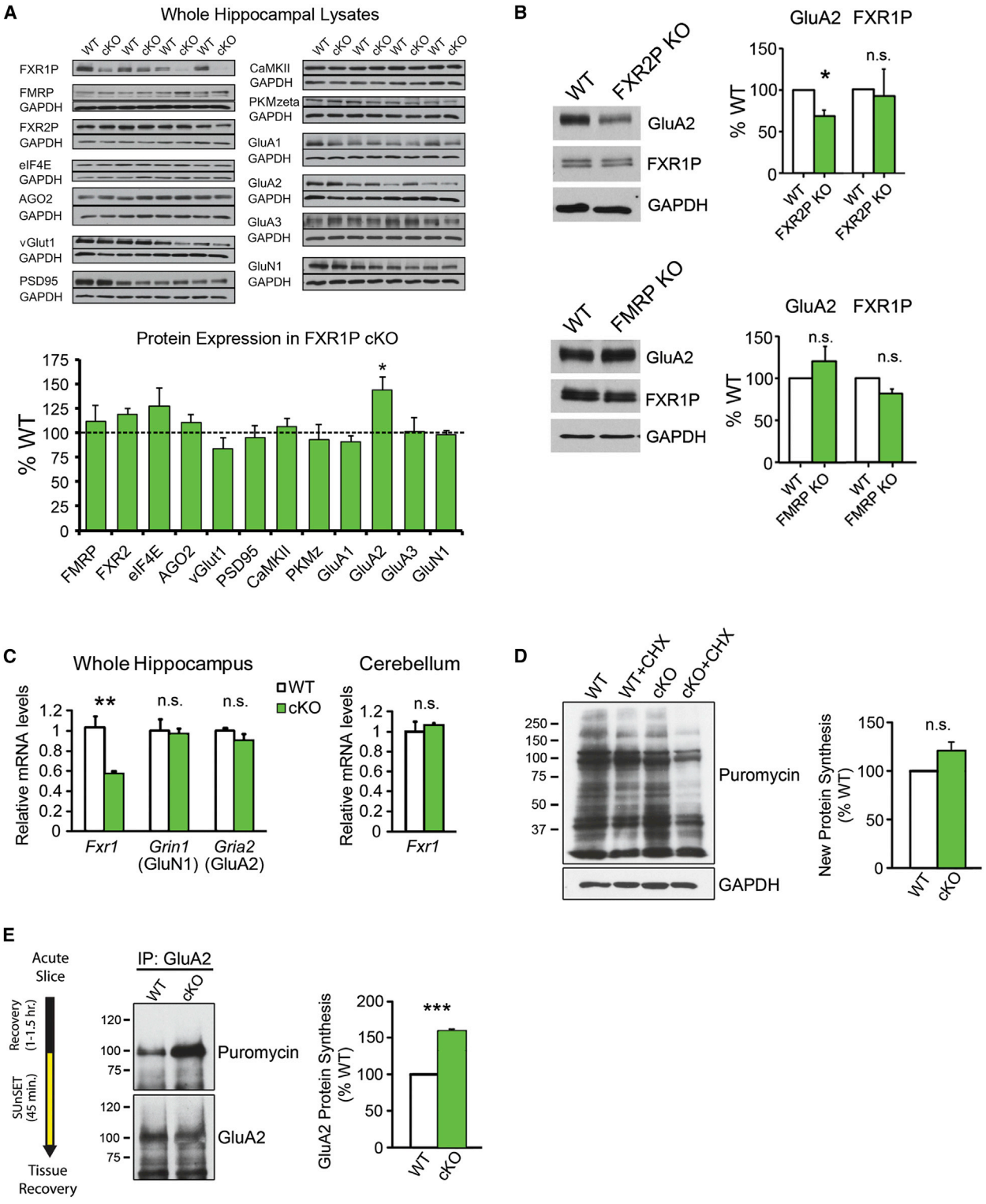

Figure 4. Enhanced GluA2 Translation in FXR1P cKO Mice

(A) Top: analysis of Fragile X family proteins, molecules involved in protein synthesis, and synaptic proteins in WT and cKO mice (four pairs of animals). Most proteins are similarly expressed in both genotypes (two-tailed, one-sample t tests; $p > 0.05$) with the exception of GluA2 (two-tailed, one-sample t test; $p = 0.02$). Each blot was run two to three times and values were averaged.

(legend continued on next page)

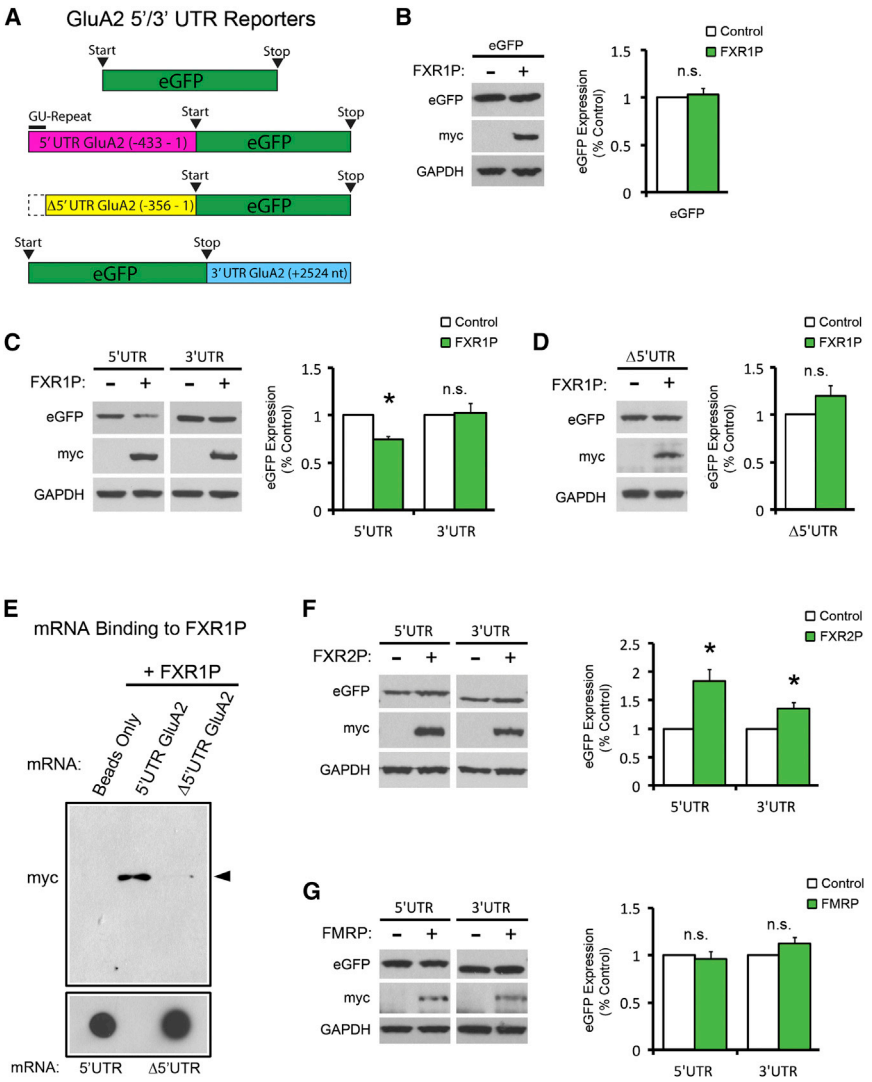

Figure 5. FXR1P Represses Translation through a GU-Rich Element in the GluA2 5′ UTR

(A) Constructs used in GluA2 reporter assay; eGFP, eGFP with the GluA2 5′ UTR (−433 to 1), eGFP with the 5′ UTR GU-rich element removed (Δ5′ UTR (−356 to 1)), and eGFP with the GluA2 3′ UTR (+2,524 nt).

(B) FXR1P does not affect expression of eGFP alone ($p = 0.62$).

(C) FXR1P represses expression from the GluA2 5′ UTR-eGFP ($p = 0.004$), but not the GluA2 eGFP-3′ UTR construct ($p = 0.84$).

(D) Deletion of the GU-rich element relieves FXR1P-mediated repression.

(E) Loss of the GU-rich element prevents binding of FXR1P to the 5′ UTR of GluA2.

(F) FXR2P increases eGFP expression from constructs containing either the GluA2 5′ UTR ($p = 0.02$) or 3′ UTR ($p = 0.05$).

(G) FMRP does not regulate expression from either construct ($p > 0.05$).

Analyses were performed using two-tailed, one-sample t tests. n = 3–4 separate cultures and transfections. Error bars show SE. *$p \leq 0.05$; n.s., not significant. See also Figure S5.

GluA1-GluA2 association was due to an enrichment of GluA2-GluA2 interactions and/or caused by a reduced amount of total synaptic GluA1, we probed unbound synaptic fractions following GluA1 or GluA2 IP (Sans et al., 2003). Blotting the unbound GluA2 IP fraction for GluA1 showed that GluA1 was not depleted from the input (Figure 7E), and in fact showed similar levels between genotypes. These results indicated that the cLTP-induced increase in GluA2-containing synaptic AMPARs in cKO slices was due to preferential GluA2-GluA2 associations. Importantly, blotting the unbound fraction for GluA2 showed that GluA2 was abundant in samples from both genotypes, confirming that the change in GluA2-GluA2 association following cLTP was not caused by an IP-mediated depletion of GluA2 from WT slices (Figure 7F). In contrast to these findings, GluA1 IP caused a depletion of GluA1 from the unbound fractions from inputs for both genotypes (Figure 7G). This suggests that the reduction in GluA2 coprecipitating with GluA1 (Figure 7D) is related to decreased GluA1-containing AMPARs at synapses in cKO slices upon cLTP. Blotting the GluA1 IP unbound fraction for GluA2 showed an increase in residual synaptic GluA2 from cKO slices (Figure 7H). These results demonstrate that FXR1P regulates GluA2 incorporation at potentiated synapses and controls activity-dependent changes in AMPAR composition.

(B) Top: blots of hippocampal lysates from WT and FXR2P KO mice showing levels of GluA2, FXR1P, and GAPDH. GluA2 is reduced (two-tailed, one-sample t test, $p = 0.05$; n = 3 WT/3 FXR2P KO mice) and FXR1P is unchanged in FXR2P KO mice (two-tailed, one-sample t test, $p = 0.26$; n = 3 WT/3 KO mice). Bottom: blots of hippocampal lysates from WT and FMRP KO mice showing levels of GluA2, FXR1P, and GAPDH. GluA2 and FXR1P are unchanged in FMRP KO mice (two-tailed, one-sample t test, $p > 0.05$; n = 3 WT/3 FMRP KO mice).

(C) qRT-PCR shows that *Fxr1* mRNA levels are reduced in hippocampal lysates from FXR1P cKO mice (two-tailed, unpaired two-sample t test, $p = 0.005$; n = 3 WT/4 cKO mice from 3 litters). The mRNA levels of *Gria2* (GluA2) and *Grin1* (GluN1) are unchanged (two-tailed, unpaired two-sample t tests, $p > 0.05$; n = 3 WT/4 cKO mice). *Fxr1* mRNA levels are unaltered in the cKO cerebellum (two-tailed, unpaired two-sample t test, $p > 0.05$; n = 3 WT/3 cKO mice from 3 litters).

(D) Puromycin-labeled lysates from WT and cKO mice in the presence or absence of CHX. No differences in overall puromycin labeling are detected between genotypes ($p > 0.05$; n = 3 WT/3 cKO mice).

(E) IP for GluA2 shows increased puromycin-labeled GluA2 in slices from cKO mice, indicating enhanced GluA2 translation ($p = 0.002$; n = 3 WT/3 cKO mice). Unless otherwise stated, statistical analyses were performed using two-tailed, one-sample t tests. Error bars show SE. ***$p \leq 0.001$, **$p \leq 0.01$, *$p \leq 0.05$; n.s., not significant. See also Figures S3 and S4.

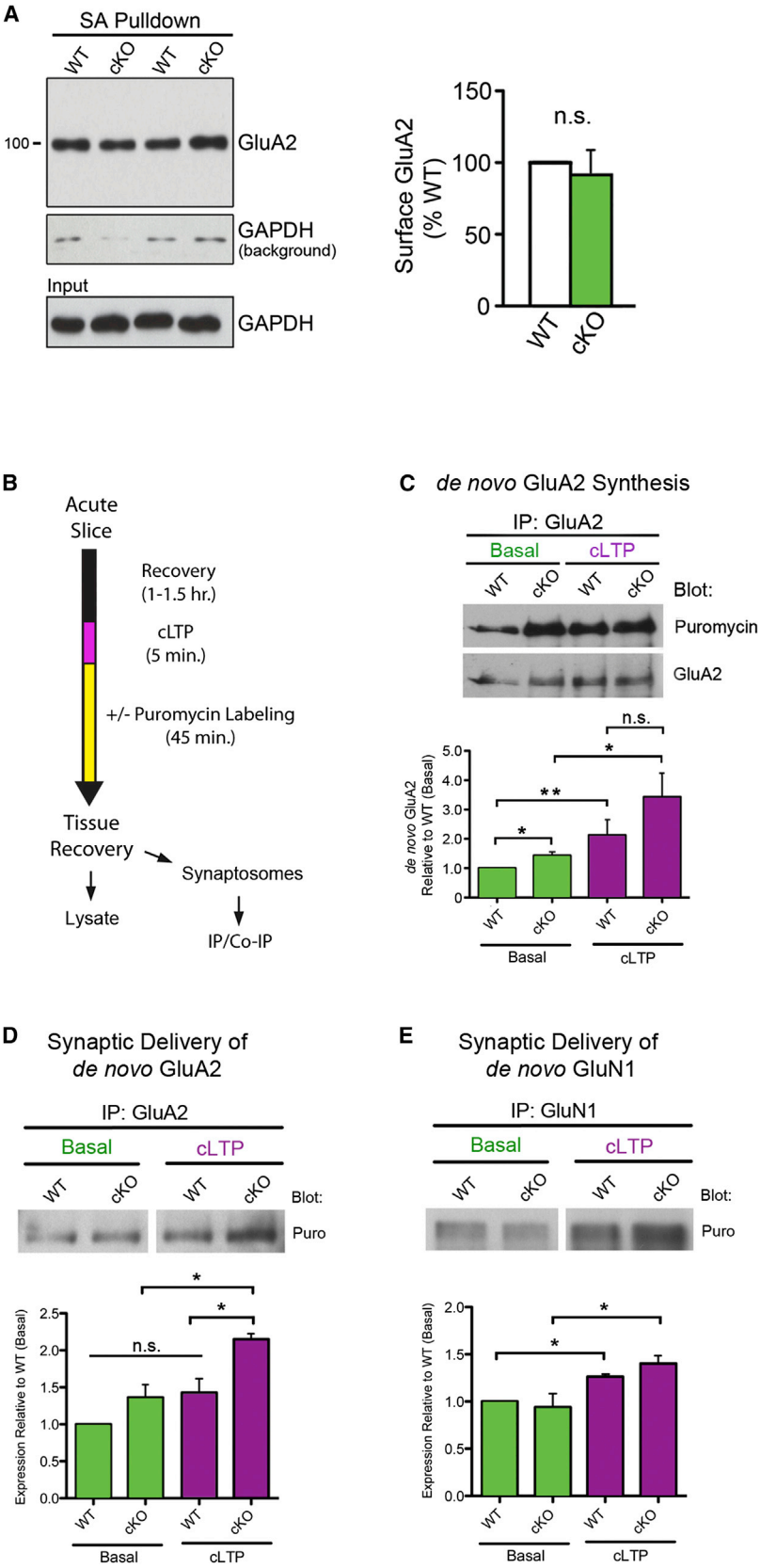

Figure 6. FXR1P Controls Activity-Dependent Synaptic Delivery of GluA2

(A) Basal surface GluA2 levels are similar between genotypes ($p = 0.66$; $n = 3$ WT/3 cKO mice). Only low levels of GAPDH were biotinylated during the surface labeling process and purified with streptavidin (SA) beads (GAPDH background).

(B) Time course for cLTP experiments.

(C) cKO slices show increased basal de novo synthesis of GluA2 ($p = 0.04$). Both WT and cKO slices increase GluA2 synthesis upon cLTP (WT: $p = 0.02$; cKO: $p = 0.05$; two-tailed, unpaired, two-sample t test).

(D) cKO slices show increases in GluA2 synaptic delivery following cLTP ($n = 3$ WT/3 cKO mice; $p = 0.01$).

(E) GluN1 synaptic delivery is similar between genotypes ($n = 3$ WT/3 cKO mice; $p > 0.05$).

Unless otherwise stated, statistical analyses were performed using two-tailed, one-sample t tests. Error bars show SE. $^{**}p \leq 0.01$, $^{*}p \leq 0.05$; n.s., not significant. See also Figure S6.

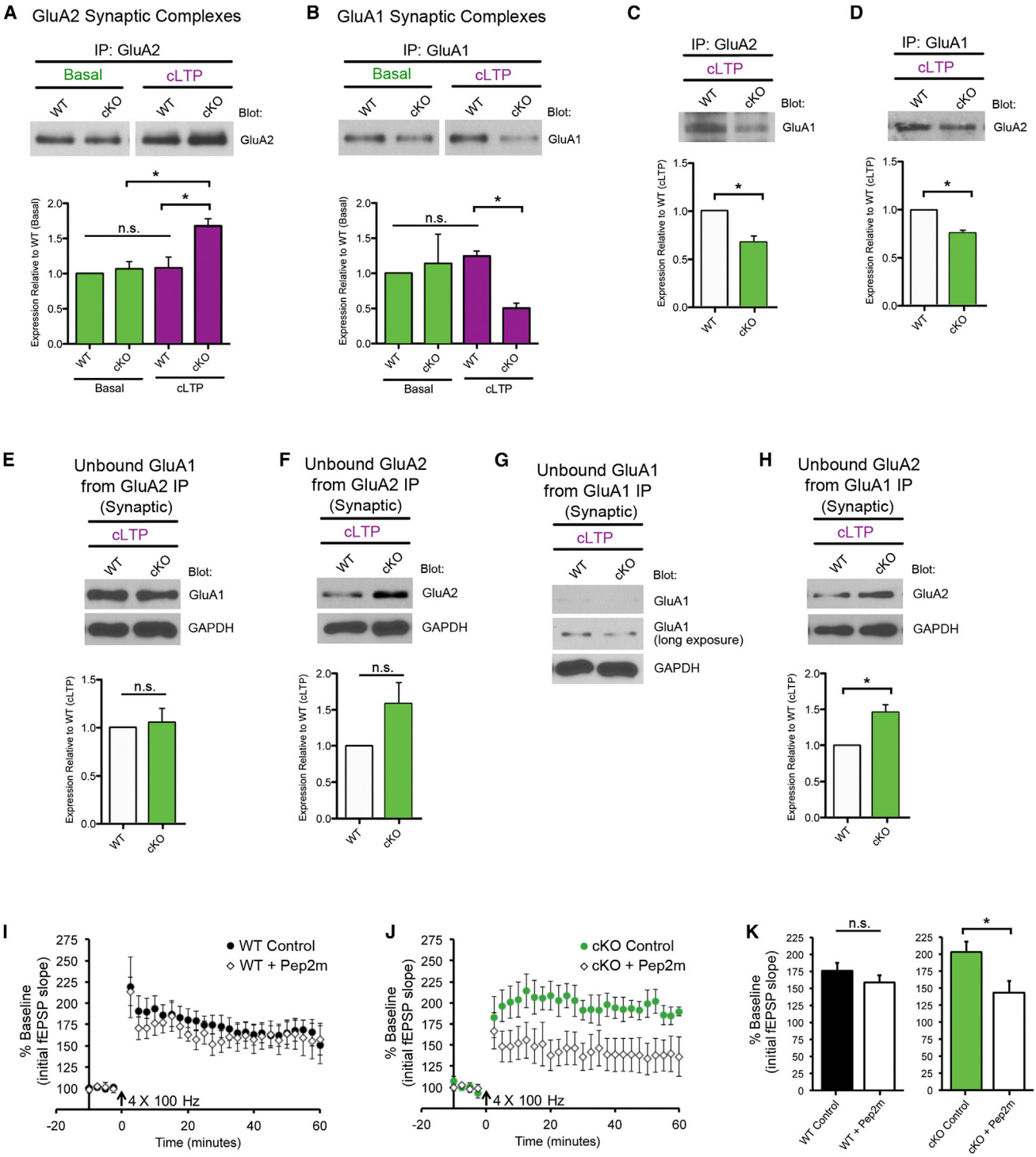

Figure 7. FXR1P Controls Activity-Dependent AMPAR Composition

(A) cKO slices show increases in GluA2-containing AMPARs at synapses following cLTP (n = 3 WT/3 cKO mice; p = 0.03).

(B) cKO slices show decreases in GluA1-containing AMPARs at synapses following cLTP (n = 3 WT/3 cKO mice; p = 0.002).

(C and D) cKO slices show decreases in association of GluA1 with GluA2 following cLTP in cKO slices (n = 3 WT/3 cKO mice; p = 0.04 and p = 0.01, respectively).

(E–H) Blotting unbound fractions from coIPs (C and D) show the amount of residual GluA1 and GluA2 molecules.

(I and J) cKO slices preincubated with myristoylated Pep2m show a significant reduction in potentiation at 20–30 min after L-LTP induction (WT (± pep2m): p = 0.36; cKO (± pep2m): p = 0.04, two-tailed, unpaired t tests).

Unless otherwise stated, statistical analyses were performed using two-tailed, one-sample t tests; *p ≤ 0.05; n.s., not significant. See also Figure S7.

Given these biochemical changes at cKO synapses, we sought to determine whether increased trafficking/stabilization of GluA2-containing receptors to synapses contributes to elevated L-LTP (Figures 3D and 3E). To that end, we preincubated WT and cKO slices with myr-Pep2m, a cell-permeable peptide that blocks GluA2 subunit trafficking and stabilization at synapses by disrupting GluA2-NSF interactions (Nishimune et al., 1998; Yao et al., 2008) and repeated the L-LTP experiments. Remarkably, preincubation of slices with myr-Pep2m caused a significant reduction in L-LTP in cKO slices, but not in WT slices (Figures 7I–7K). Thus, enhanced trafficking or stabilization of GluA2-containing receptors at synapses contributes to elevated L-LTP in cKO mice.

DISCUSSION

For long-term synaptic plasticity and memory formation to occur properly, new proteins must be synthesized in a temporally and spatially precise manner in response to specific patterns of activity, a process that is tightly controlled at the level of mRNA translation. We have identified the RNA-binding protein FXR1P as a key player in controlling specific aspects of synaptic protein expression, synaptic plasticity, and memory formation. Loss of FXR1P enhances synthesis of GluA2, increases delivery of GluA2 to potentiated synapses, heightens L-LTP, and improves long-term memory storage. Mechanistically, FXR1P utilizes the GU-rich element in the GluA2 5′ UTR to repress translation. These findings define a molecular pathway that regulates distinct features of synaptic plasticity and cognitive function.

This study also addresses a long-standing issue in the protein translation field regarding how the three Fragile X protein family members (FMRP, FXR1P, and FXR2P) functionally relate to each other (Bontekoe et al., 2002). All three proteins associate with polyribosomes and messenger ribonucleoprotein particles (mRNPs), are found at spines, and are expressed in similar patterns in the brain, raising the question as to whether they perform redundant functions (Cook et al., 2014; Tamanini et al., 1997, 2000). However, until now, nothing was known about the mRNA targets of FXR1P or its role in the brain. We provide several lines of evidence demonstrating the functional divergence of FXR1P from FMRP and FXR2P in synaptic plasticity, behavior, spine development, and GluA2 translational control. First, whereas FMRP and FXR2P function predominantly in hippocampal mGluR-LTD (Zhang et al., 2009), FXR1P participates selectively in L-LTP. Second, FXR1P cKO mice display improved long-term spatial memory, whereas FMRP and FXR2P KO animals show memory impairments (Bontekoe et al., 2002; Kooy et al., 1996). Third, loss of FXR1P reduces spine density and spine size, whereas loss of FMRP increases spine density and length. Lastly, FXR1P represses GluA2 translation, whereas FXR2P enhances it and FMRP has no major effect. Overall, our work reveals a unique function for FXR1P and offers a clear demonstration of the differential role of Fragile X proteins in brain plasticity. In future studies, it may be of interest to explore the combinatorial role of this family of mRNA-binding proteins in plasticity by using double cKO models of FXR1P/FMRP and FXR1P/FXR2P.

An intriguing finding is the specificity of the FXR1P cKO behavioral phenotype. Although cKO mice performed normally in the majority of behavioral paradigms, they demonstrated a specific improvement in long-term spatial memory and alteration in behavioral flexibility. Most revealing is the observation that cKOs showed greater long-term memory recall 9 days after the initial training and a similar preference for new and old platform locations during the reversal probe test, suggesting that cKO mice maintain stronger memories that allow them to keep multiple memories "online" when performing a task. This phenotype is striking considering that mutant mice with alterations in general protein synthesis pathway components commonly show impairments in long-term memory (Costa-Mattioli et al., 2005, 2007; Kelleher et al., 2004) or, in some cases, increased perseverative behavior (Hoeffer et al., 2008; Trinh et al., 2012). The fact that cKO mice readily learn a new platform location suggests that they do not perseverate in this task; rather, they maintain and retrieve multiple spatial memory traces and are able to more rapidly and efficiently shift between memory stores based on changing performance demands (i.e., platform removal during the reversal probe trial). By constraining the magnitude of long-lasting increases in synaptic strength, FXR1P may control the extent of information storage in brain circuits.

Remarkably, among the synaptic proteins we screened, FXR1P only affected the protein synthesis of GluA2. This is surprising in light of the fact that FMRP binds ~800 brain mRNAs (Darnell et al., 2011), associates with diverse RNA cargoes (Ascano et al., 2012; Miyashiro et al., 2003), and controls translation initiation of multiple targets through eIF4E (Napoli et al., 2008). Although we cannot rule out the possibility that FXR1P also regulates other proteins, GluA2 is an interesting target because it is present at the majority of brain excitatory synapses, confers calcium impermeability to AMPARs, and is critical for long-lasting synaptic plasticity and spatial memories (Isaac et al., 2007; Migues et al., 2010; Yao et al., 2008). Furthermore, GluA2 is known to be regulated at the level of mRNA translation, although exactly how this is accomplished is unknown. Our results indicate that FXR1P binds and represses translation of transcripts with the long 5′ UTR of GluA2 containing a GU-rich element that is predicted to form a stem-loop structure that interferes with translation initiation (Myers et al., 2004). Notably, this GU-rich repeat is present in human GluA2 transcripts, causing a 2.5- to 3-fold reduction in GluA2 translation efficiency (Myers et al., 2004). Translational control of GluA2 mRNA through the GU-rich sequence by FXR1P may be a conserved mechanism for carefully titrating the amount of long-lasting synaptic plasticity and memory storage in the brain.

Interestingly, a basal increase in GluA2 mRNA translation in FXR1P cKO mice is not accompanied by baseline increases in its surface levels, synaptic incorporation, or synaptic transmission. This indicates that neurons in cKO mice have a larger internal reserve of GluA2 that is specifically mobilized to synapses during protein synthesis-dependent plasticity such as L-LTP. Baseline phosphorylation of GluA1 S845, but not total levels of GluA1, is also enhanced in cKO mice. The reason for this modification is unclear. However, as pS845 promotes trafficking of GluA1-containing AMPARs to extrasynaptic and perisynaptic sites, this alteration in cKO mice may further promote the exchange of GluA2 for GluA1 at synapses and increase the ability of GluA2-containing AMPARs to compete for synaptic territory

during L-LTP. Remarkably, the enhancement in synaptic strength in the cKO mice is revealed only by a strong stimulus that elicits protein synthesis-dependent L-LTP, and not by a stimulus that promotes E-LTP. Thus, the activity-dependent production or modification of facilitatory proteins is still required to mobilize the reserve pool of GluA2 to synapses. Furthermore, elevations of L-LTP in cKO mice can be suppressed by blocking GluA2 trafficking or stabilization at the synapse with myr-Pep2m, a peptide that blocks GluA2-NSF interactions. This result further supports the increased role played by GluA2-containing receptors in L-LTP. The increased size of the GluA2 reserve pool in cKO mice may enable more rapid stabilization of L-LTP and better maintenance of memories (Kelz et al., 1999; Migues et al., 2010; Yao et al., 2008). These findings align with discoveries showing that the size of the AMPAR reserve pool is important for LTP (Granger et al., 2013) and provide an in vivo demonstration of an endogenous GluA2 gain-of-function effect on synaptic properties. Interestingly, SNPs in glutamate receptor interacting protein 1 (GRIP1) that promote GluA2 surface stabilization in neurons are associated with autism (Mejias et al., 2011), further implicating synaptic GluA2 levels in regulating cognitive function. Future studies will need to dissect the molecular network surrounding FXR1P and further elucidate its role in modifying brain plasticity states.

EXPERIMENTAL PROCEDURES

Animals

Experiments were approved by the Montreal General Hospital Facility Animal Care Committee and followed the guidelines of the Canadian Council on Animal Care. Both male and female mice were used for experiments. All mice were kept on a standard 12 hr light/dark cycle and socially housed (n = 2–5 animals per cage).

FXR1P cKO Mice

Floxed *Fxr1* mice (Fragile-X Mutant Mouse Facility, Baylor College of Medicine) were crossed into the αCaMKII-Cre T29-1 Cre-recombinase driver line (The Jackson Laboratory) (Sonner et al., 2005; Tsien et al., 1996). Experimental animals were generated by crossing αCaMKII-Cre tg/tg; *Fxr1* fl/+ mice with *Fxr1* fl/+ mice to generate αCaMKII-Cre tg/+; *Fxr1* fl/fl (FXR1P cKO), αCaMKII-Cre tg/+; *Fxr1* fl/+ (FXR1P cHET), and αCaMKII-Cre tg/+; *Fxr1* +/+ (WT). These lines were backcrossed into C57BL/6 for at least ten generations. To track cells that had undergone Cre-mediated recombination, we crossed αCaMKII-Cre tg/tg; *Fxr1* fl/+ mice with the mTom/mGFP reporter line (The Jackson Laboratory) (Muzumdar et al., 2007). The reporter line was backcrossed into a C57BL/6 background for at least five generations.

FMRP and FXR2P KO Mice

Whole hippocampal tissue from C57BL/6 background *Fmr1* KO and *Fxr2* KO adult mice (>7 weeks old) was provided by the David L. Nelson laboratory. Lysates were prepared and processed for western blotting as previously described (Cook et al., 2011).

Plasmids

The 5′ UTR (−433-1) and 3′ UTR (+2524nt) GluA2 eGFP constructs were described previously (La Via et al., 2013). The 5′ UTR GU mutant (deletion of 65 bases from −429 to −365 containing the GU-repeat region) was generated using the existing restriction sites *Bss*HII and *Nhe*I as described previously (Irier et al., 2009).

Immunohistochemistry, DiI Labeling of CA1 Dendrites, and Imaging

Perfusion, cryostat sectioning, and imaging were performed as previously described (Cook et al., 2011). See Supplemental Experimental Procedures for details on DiI labeling and antibodies.

Whole Hippocampal and CA1 Lysates and Western Blotting

Whole hippocampal and CA1 lysates were prepared and processed for western blotting as previously described (Cook et al., 2011). See Supplemental Experimental Procedures for details on the antibodies used.

Polysome Fractionation

Experiments were performed on 13- to 16-week-old mice as previously described (Gandin et al., 2014). EDTA (200 μg/ml) was added to the lysis buffer to disrupt polysomes.

Behavior

Behavioral assessments were performed between 9:00 a.m. and 3:00 p.m. on 2- to 6-month-old mice by an investigator blind to genotype. A period of acclimatization to the environment (10–15 min) preceded all experiments. Four separate cohorts of mice were tested on the Morris water maze, object-recognition test, and fear-conditioning tests (in that order), with at least 72 hr between the beginning and end of each new paradigm. Mice from cohorts 3 and 4 were subsequently used in field recording experiments. Mice that were tested in both the open-field and dark/light box tests were allowed at least 1 week between the two behavioral paradigms. Besides the differences in behavioral phenotypes reported in Figure 2, no other phenotypic changes were observed. See Supplemental Experimental Procedures for additional details regarding each of the behavioral paradigms used.

Electrophysiology

Standard procedures were used for field excitatory postsynaptic potential (fEPSP) recordings. Mice (5–9 months old, used previously in behavioral testing) were anesthetized with isoflurane and quickly decapitated. The whole brain was immersed in ice-cold ACSF (in mM: NaCl 124, KCl 3, NaH_2PO_4 1.25, $CaCl_2$ 2, $MgSO_4$ 1, $NaHCO_3$ 26, D-Glucose 10) and saturated with 95% O_2/5% CO_2. Coronal slices (300–400 μm thick) were cut with a Leica VT1200S and transferred to a submersion chamber containing regular ACSF at a temperature of 32–37°C for 25–30 min, after which the chamber was placed on the bench at room temperature. The slices were allowed to recover in the submersion chamber for at least 4 hr (Sajikumar et al., 2005). After the recovery period, the slices were transferred to a submersion chamber mounted on an electrophysiology rig, perfused with regular ACSF (3 ml/min), and maintained at 28°C–31°C. Field synaptic responses were evoked by stimulating Schaffer collaterals with 0.1 ms pulses delivered at 0.033–0.067 Hz and recorded extracellularly in CA1 stratum radiatum. Input-output curves were generated by stimulation at different intensities (n = 18 WT mice from 11 litters, n = 19 cKO mice from 11 litters). For all subsequent experiments, the stimulation intensity was set to elicit an fEPSP with a slope that was approximately 40% of the maximum obtained slope. Paired-pulse facilitation was determined by delivering pulses at varying interpulse intervals (n = 7 WT mice from 6 litters, n = 8 cKO mice from 6 litters). E-LTP was induced with a single train of HFS (1 × 100 Hz) using the baseline stimulation intensity (n = 10 mice, 12 slices, from 5 litters). L-LTP was induced using four trains of HFS with a 20 s interval (4 × 100 Hz) using baseline stimulation intensity (n = 7 mice, 7 slices, from 5 litters). For mGluR-LTD induction, slices from 5- to 9-week-old mice were perfused for 7–8 min with DHPG (100 μM) and the initial stimulation was kept at 0.5 mV (n = 4 mice, 8 slices for WT; n = 6 mice, 8 slices for cKO). For GluA2-NSF disruption experiments, slices from 3.5- to 6-month-old mice were incubated for at least 1 hr with myristoylated-pep2m (100 μM; Tocris) in ACSF and then switched to normal ACSF for baseline recordings and L-LTP (n = 5 mice, 5 slices for WT control; n = 4 mice, 7 slices for WT pep2m, n = 4 mice, 5 slices cKO control; n = 5 mice, 5 slices for cKO pep2m). To reduce the possibility of rundown of basal responses by pep2m, test stimulations were given every 15 s as described previously (Yao et al., 2008).

Real-Time qRT-PCR

Standard methods were used for qRT-PCR. More information on qRT-PCR can be found in Supplemental Experimental Procedures.

GluA2 Reporter Assays and FXR1P Binding to the GluA2 5′ UTR

For information on GluA2 reporter assays and FXR1P binding to the GluA2 5′ UTR, see Supplemental Experimental Procedures.

SUnSET Labeling of Newly Synthesized Proteins and IP Assays

Adult mice (>12 weeks old) were deeply anesthetized with isoflurane in an enclosed chamber and decapitated. The brain was quickly removed and immersed in ice-cold ACSF containing (in mM) 119 choline-Cl, 2.5 KCl, 4.3 $MgSO_4$, 1.0 NaH_2PO_4, 1.0 $CaCl_2$, 1.30 Na-ascorbate, 11 glucose, and 26.2 $NaHCO_3$, continuously bubbled with 95% O_2 and 5% CO_2 (pH 7.4). Coronal slices (400 μm) containing the hippocampus were obtained with a vibratome. Slices (three or four per condition) were recovered at room temperature for 1–1.5 hr in oxygenated ACSF with the following composition (in mM): 119 NaCl, 2.5 KCl, 1.3 $MgSO_4$, 1.0 NaH_2PO_4, 2.5 $CaCl_2$, 11 glucose, and 26.2 $NaHCO_3$ (pH 7.4). SUnSET (Schmidt et al., 2009) was then used to probe for newly synthesized proteins. Briefly, slices were incubated with puromycin (5 μg/ml) for 45 min. Control slices were incubated first with cycloheximide (CHX) (20 μg/ml, C7698; Sigma-Aldrich) for 30 min and then with puromycin plus CHX for 45 min. Following the incubation, the tissue was snap-frozen using either dry ice or liquid nitrogen. The tissue was then lysed (RIPA lysis buffer) and prepared for western blot or IP with GluA2 antibodies. GluA2 immunoprecipitates were blotted for puromycin, stripped, and reprobed for GluA2. The level of puromycin-labeled GluA2 was normalized to the amount of immunoprecipitated GluA2. For analysis of the synaptic GluA1/GluA2 AMPA receptor complex, after puromycin incubation, the tissue was lysed in Syn-PER Synaptic Protein extraction Reagent (Thermo Scientific #87793) and the synaptosomal fraction was extracted according to the supplier's directions. Following synaptosomal purification, coIP experiments for GluA1 and GluA2 were carried out according to a previously published protocol (Kang et al., 2012). Coimmunoprecipitated lysate and the unbound fraction from the coIP were blotted for GluA2 and GluA1 using anti-GluA2 and anti-GluA1 antibodies.

cLTP

The cLTP methods were adapted from previously published studies (Huang and Kandel, 1994; Otmakhov et al., 2004). Briefly, coronal slices (prepared as mentioned above) were incubated for 5 min in oxygenated ACSF (low Mg^{2+}, 0.13 mM) with forskolin (F6886 Sigma-Aldrich; 50 μM dissolved in DMSO). Slices were then transferred into oxygenated ACSF containing puromycin (P8833 Sigma-Aldrich; 5 μg/ml) and incubated for 45 min. For the control group, slices were incubated with DMSO (50 μM) in regular ACSF for 5 min and then incubated in puromycin for 45 min. The slices were then processed for western blotting or IP as described above.

Surface Biotinylation Assays

To investigate cell-surface expression of GluA2, a tissue chopper was used to obtain transverse hippocampal sections (300 μm) from adult mice (>8 weeks old). The sections were incubated with biotin (1 mg/ml in PBS) solution for 30–40 min at 4°C and then homogenized with lysis buffer (PBS/0.1% SDS/10% glycerol). Upon homogenization, the lysate was incubated with streptavidin beads (50 μl/sample prewashed with PBS) for 1 hr and then prepared for western blotting. For analysis of the activity-dependent surface GluA2 receptor, after cLTP induction, tissue was incubated at 4°C in bubbling ACSF with biotin for 45 min. The tissue was then snap-frozen using dry ice, lysed, and incubated with streptavidin beads (50 μl/sample prewashed with PBS) for 1 hr and then prepared for western blotting.

Statistical Analysis

Analyses were performed using R (http://www.R-project.org) with the Reshape, Hmisc, gplots, plotrix, ezANOVA, and Microsoft Excel packages; $\alpha = 0.05$ was chosen for statistical significance. The tests used are noted in the figure legends. Analyses were collapsed across sex to reflect the fact that preliminary ANOVAs demonstrated no sex effect. All graphs were created using R or Microsoft Excel.

SUPPLEMENTAL INFORMATION

Supplemental Information includes Supplemental Experimental Procedures and seven figures and can be found with this article online at http://dx.doi.org/10.1016/j.celrep.2014.10.028.

AUTHOR CONTRIBUTIONS

D.C., E.N., and K.K.M. designed experiments, analyzed data, and wrote the manuscript. D.C. established the FXR1P cKO line and performed experiments and analyzed data for Figures 1, 2, 3, S1, and S2. E.N. performed experiments and analyzed data for Figures 4, 6, 7, S3, S4, S6, and S7.

ACKNOWLEDGMENTS

The authors thank Dr. E. Khandjian (Laval University) for the FXR1P antibody, P. Thandapani for help with the mRNA binding studies, and E.M. Charbonneau for expert technical work on the behavioral studies. This work was supported by the Canadian Institutes of Health Research (CHIR; MOP111152 and MOP123390 to K.K.M.), the Natural Sciences and Engineering Research Council of Canada (RGPIN-408044-11 to K.K.M.), and the NIH (1R21DA026053-01 to K.K.M. and D.S.). I.T. received a CIHR Young Investigator Award and a grant from the FRQS (Subvention Établissement de Jeunes Chercheurs). D.C. was supported through doctoral awards from the CIHR and FRQS. E.N. and H.F.A. were supported by awards from the Integrated Program in Neuroscience at McGill University and the Heart and Stroke Foundation of Canada, respectively.

Received: May 29, 2014
Revised: August 28, 2014
Accepted: October 11, 2014
Published: November 13, 2014

REFERENCES

Ascano, M., Jr., Mukherjee, N., Bandaru, P., Miller, J.B., Nusbaum, J.D., Corcoran, D.L., Langlois, C., Munschauer, M., Dewell, S., Hafner, M., et al. (2012). FMRP targets distinct mRNA sequence elements to regulate protein expression. Nature *492*, 382–386.

Bontekoe, C.J.M., McIlwain, K.L., Nieuwenhuizen, I.M., Yuva-Paylor, L.A., Nellis, A., Willemsen, R., Fang, Z., Kirkpatrick, L., Bakker, C.E., McAninch, R., et al. (2002). Knockout mouse model for Fxr2: a model for mental retardation. Hum. Mol. Genet. *11*, 487–498.

Cook, D., Sanchez-Carbente, M. del R., Lachance, C., Radzioch, D., Tremblay, S., Khandjian, E.W., DesGroseillers, L., and Murai, K.K. (2011). Fragile X related protein 1 clusters with ribosomes and messenger RNAs at a subset of dendritic spines in the mouse hippocampus. PLoS ONE *6*, e26120.

Cook, D., Nuro, E., and Murai, K.K. (2014). Increasing our understanding of human cognition through the study of Fragile X Syndrome. Dev. Neurobiol. *74*, 147–177.

Costa-Mattioli, M., Gobert, D., Harding, H., Herdy, B., Azzi, M., Bruno, M., Bidinosti, M., Ben Mamou, C., Marcinkiewicz, E., Yoshida, M., et al. (2005). Translational control of hippocampal synaptic plasticity and memory by the eIF2alpha kinase GCN2. Nature *436*, 1166–1173.

Costa-Mattioli, M., Gobert, D., Stern, E., Gamache, K., Colina, R., Cuello, C., Sossin, W., Kaufman, R., Pelletier, J., Rosenblum, K., et al. (2007). eIF2alpha phosphorylation bidirectionally regulates the switch from short- to long-term synaptic plasticity and memory. Cell *129*, 195–206.

Costa-Mattioli, M., Sossin, W.S., Klann, E., and Sonenberg, N. (2009). Translational control of long-lasting synaptic plasticity and memory. Neuron *61*, 10–26.

Darnell, J.C., Van Driesche, S.J., Zhang, C., Hung, K.Y.S., Mele, A., Fraser, C.E., Stone, E.F., Chen, C., Fak, J.J., Chi, S.W., et al. (2011). FMRP stalls ribosomal translocation on mRNAs linked to synaptic function and autism. Cell *146*, 247–261.

Dobrunz, L.E., and Stevens, C.F. (1997). Heterogeneity of release probability, facilitation, and depletion at central synapses. Neuron *18*, 995–1008.

Doyle, M., and Kiebler, M.A. (2011). Mechanisms of dendritic mRNA transport and its role in synaptic tagging. EMBO J. *30*, 3540–3552.

Elvira, G., Wasiak, S., Blandford, V., Tong, X.-K., Serrano, A., Fan, X., del Rayo Sánchez-Carbente, M., Servant, F., Bell, A.W., Boismenu, D., et al. (2006).

Characterization of an RNA granule from developing brain. Mol. Cell. Proteomics *5*, 635–651.

Gandin, V., Sikström, K., Alain, T., Morita, M., McLaughlan, S., Larsson, O., and Topisirovic, I. (2014). Polysome fractionation and analysis of mammalian translatomes on a genome-wide scale. J. Vis. Exp. (87), e51455.

Garnon, J., Lachance, C., Di Marco, S., Hel, Z., Marion, D., Ruiz, M.C., Newkirk, M.M., Khandjian, E.W., and Radzioch, D. (2005). Fragile X-related protein FXR1P regulates proinflammatory cytokine tumor necrosis factor expression at the post-transcriptional level. J. Biol. Chem. *280*, 5750–5763.

Govindarajan, A., Kelleher, R.J., and Tonegawa, S. (2006). A clustered plasticity model of long-term memory engrams. Nat. Rev. Neurosci. *7*, 575–583.

Granger, A.J., Shi, Y., Lu, W., Cerpas, M., and Nicoll, R.A. (2013). LTP requires a reserve pool of glutamate receptors independent of subunit type. Nature *493*, 495–500.

Hershey, J.W.B., Sonenberg, N., and Mathews, M.B. (2012). Principles of translational control: an overview. Cold Spring Harb. Perspect. Biol. *4*, pii: a011528.

Hoeffer, C.A., Tang, W., Wong, H., Santillan, A., Patterson, R.J., Martinez, L.A., Tejada-Simon, M.V., Paylor, R., Hamilton, S.L., and Klann, E. (2008). Removal of FKBP12 enhances mTOR-Raptor interactions, LTP, memory, and perseverative/repetitive behavior. Neuron *60*, 832–845.

Huang, Y.Y., and Kandel, E.R. (1994). Recruitment of long-lasting and protein kinase A-dependent long-term potentiation in the CA1 region of hippocampus requires repeated tetanization. Learn. Mem. *1*, 74–82.

Huber, K.M., Gallagher, S.M., Warren, S.T., and Bear, M.F. (2002). Altered synaptic plasticity in a mouse model of fragile X mental retardation. Proc. Natl. Acad. Sci. USA *99*, 7746–7750.

Irier, H.A., Quan, Y., Yoo, J., and Dingledine, R. (2009). Control of glutamate receptor 2 (GluR2) translational initiation by its alternative 3′ untranslated regions. Mol. Pharmacol. *76*, 1145–1149.

Isaac, J.T.R., Ashby, M.C., and McBain, C.J. (2007). The role of the GluR2 subunit in AMPA receptor function and synaptic plasticity. Neuron *54*, 859–871.

Kanai, Y., Dohmae, N., and Hirokawa, N. (2004). Kinesin transports RNA: isolation and characterization of an RNA-transporting granule. Neuron *43*, 513–525.

Kang, M.-G., Nuriya, M., Guo, Y., Martindale, K.D., Lee, D.Z., and Huganir, R.L. (2012). Proteomic analysis of α-amino-3-hydroxy-5-methyl-4-isoxazole propionate receptor complexes. J. Biol. Chem. *287*, 28632–28645.

Kelleher, R.J., 3rd, Govindarajan, A., Jung, H.-Y., Kang, H., and Tonegawa, S. (2004). Translational control by MAPK signaling in long-term synaptic plasticity and memory. Cell *116*, 467–479.

Kelz, M.B., Chen, J., Carlezon, W.A., Jr., Whisler, K., Gilden, L., Beckmann, A.M., Steffen, C., Zhang, Y.J., Marotti, L., Self, D.W., et al. (1999). Expression of the transcription factor deltaFosB in the brain controls sensitivity to cocaine. Nature *401*, 272–276.

Kessels, H.W., and Malinow, R. (2009). Synaptic AMPA receptor plasticity and behavior. Neuron *61*, 340–350.

Kooy, R.F., D'Hooge, R., Reyniers, E., Bakker, C.E., Nagels, G., De Boulle, K., Storm, K., Clincke, G., De Deyn, P.P., Oostra, B.A., and Willems, P.J. (1996). Transgenic mouse model for the fragile X syndrome. Am. J. Med. Genet. *64*, 241–245.

La Via, L., Bonini, D., Russo, I., Orlandi, C., Barlati, S., and Barbon, A. (2013). Modulation of dendritic AMPA receptor mRNA trafficking by RNA splicing and editing. Nucleic Acids Res. *41*, 617–631.

Lee, H.K., Barbarosie, M., Kameyama, K., Bear, M.F., and Huganir, R.L. (2000). Regulation of distinct AMPA receptor phosphorylation sites during bidirectional synaptic plasticity. Nature *405*, 955–959.

Lu, W., Shi, Y., Jackson, A.C., Bjorgan, K., During, M.J., Sprengel, R., Seeburg, P.H., and Nicoll, R.A. (2009). Subunit composition of synaptic AMPA receptors revealed by a single-cell genetic approach. Neuron *62*, 254–268.

Man, H.-Y., Sekine-Aizawa, Y., and Huganir, R.L. (2007). Regulation of alpha-amino-3-hydroxy-5-methyl-4-isoxazolepropionic acid receptor trafficking through PKA phosphorylation of the Glu receptor 1 subunit. Proc. Natl. Acad. Sci. USA *104*, 3579–3584.

Mejias, R., Adamczyk, A., Anggono, V., Niranjan, T., Thomas, G.M., Sharma, K., Skinner, C., Schwartz, C.E., Stevenson, R.E., Fallin, M.D., et al. (2011). Gain-of-function glutamate receptor interacting protein 1 variants alter GluA2 recycling and surface distribution in patients with autism. Proc. Natl. Acad. Sci. USA *108*, 4920–4925.

Mientjes, E.J., Willemsen, R., Kirkpatrick, L.L., Nieuwenhuizen, I.M., Hoogeveen-Westerveld, M., Verweij, M., Reis, S., Bardoni, B., Hoogeveen, A.T., Oostra, B.A., and Nelson, D.L. (2004). Fxr1 knockout mice show a striated muscle phenotype: implications for Fxr1p function in vivo. Hum. Mol. Genet. *13*, 1291–1302.

Migues, P.V., Hardt, O., Wu, D.C., Gamache, K., Sacktor, T.C., Wang, Y.T., and Nader, K. (2010). PKMzeta maintains memories by regulating GluR2-dependent AMPA receptor trafficking. Nat. Neurosci. *13*, 630–634.

Miyashiro, K.Y., Beckel-Mitchener, A., Purk, T.P., Becker, K.G., Barret, T., Liu, L., Carbonetto, S., Weiler, I.J., Greenough, W.T., and Eberwine, J. (2003). RNA cargoes associating with FMRP reveal deficits in cellular functioning in Fmr1 null mice. Neuron *37*, 417–431.

Muzumdar, M.D., Tasic, B., Miyamichi, K., Li, L., and Luo, L. (2007). A global double-fluorescent Cre reporter mouse. Genesis *45*, 593–605.

Myers, S.J., Huang, Y., Genetta, T., and Dingledine, R. (2004). Inhibition of glutamate receptor 2 translation by a polymorphic repeat sequence in the 5′-untranslated leaders. J. Neurosci. *24*, 3489–3499.

Napoli, I., Mercaldo, V., Boyl, P.P., Eleuteri, B., Zalfa, F., De Rubeis, S., Di Marino, D., Mohr, E., Massimi, M., Falconi, M., et al. (2008). The fragile X syndrome protein represses activity-dependent translation through CYFIP1, a new 4E-BP. Cell *134*, 1042–1054.

Nayak, A., Zastrow, D.J., Lickteig, R., Zahniser, N.R., and Browning, M.D. (1998). Maintenance of late-phase LTP is accompanied by PKA-dependent increase in AMPA receptor synthesis. Nature *394*, 680–683.

Nishimune, A., Isaac, J.T., Molnar, E., Noel, J., Nash, S.R., Tagaya, M., Collingridge, G.L., Nakanishi, S., and Henley, J.M. (1998). NSF binding to GluR2 regulates synaptic transmission. Neuron *21*, 87–97.

Oh, M.C., Derkach, V.A., Guire, E.S., and Soderling, T.R. (2006). Extrasynaptic membrane trafficking regulated by GluR1 serine 845 phosphorylation primes AMPA receptors for long-term potentiation. J. Biol. Chem. *281*, 752–758.

Otmakhov, N., Tao-Cheng, J.-H., Carpenter, S., Asrican, B., Dosemeci, A., Reese, T.S., and Lisman, J. (2004). Persistent accumulation of calcium/calmodulin-dependent protein kinase II in dendritic spines after induction of NMDA receptor-dependent chemical long-term potentiation. J. Neurosci. *24*, 9324–9331.

Sajikumar, S., Navakkode, S., and Frey, J.U. (2005). Protein synthesis-dependent long-term functional plasticity: methods and techniques. Curr. Opin. Neurobiol. *15*, 607–613.

Sans, N., Vissel, B., Petralia, R.S., Wang, Y.-X., Chang, K., Royle, G.A., Wang, C.Y., O'Gorman, S., Heinemann, S.F., and Wenthold, R.J. (2003). Aberrant formation of glutamate receptor complexes in hippocampal neurons of mice lacking the GluR2 AMPA receptor subunit. J. Neurosci. *23*, 9367–9373.

Scharf, M.T., Woo, N.H., Lattal, K.M., Young, J.Z., Nguyen, P.V., and Abel, T. (2002). Protein synthesis is required for the enhancement of long-term potentiation and long-term memory by spaced training. J. Neurophysiol. *87*, 2770–2777.

Schmidt, E.K., Clavarino, G., Ceppi, M., and Pierre, P. (2009). SUnSET, a nonradioactive method to monitor protein synthesis. Nat. Methods *6*, 275–277.

Schuman, E.M., Dynes, J.L., and Steward, O. (2006). Synaptic regulation of translation of dendritic mRNAs. J. Neurosci. *26*, 7143–7146.

Sonner, J.M., Cascio, M., Xing, Y., Fanselow, M.S., Kralic, J.E., Morrow, A.L., Korpi, E.R., Hardy, S., Sloat, B., Eger, E.I., 2nd, and Homanics, G.E. (2005). Alpha 1 subunit-containing GABA type A receptors in forebrain contribute to the effect of inhaled anesthetics on conditioned fear. Mol. Pharmacol. *68*, 61–68.

Tamanini, F., Willemsen, R., van Unen, L., Bontekoe, C., Galjaard, H., Oostra, B.A., and Hoogeveen, A.T. (1997). Differential expression of FMR1,

FXR1 and FXR2 proteins in human brain and testis. Hum. Mol. Genet. *6*, 1315–1322.

Tamanini, F., Kirkpatrick, L.L., Schonkeren, J., van Unen, L., Bontekoe, C., Bakker, C., Nelson, D.L., Galjaard, H., Oostra, B.A., and Hoogeveen, A.T. (2000). The fragile X-related proteins FXR1P and FXR2P contain a functional nucleolar-targeting signal equivalent to the HIV-1 regulatory proteins. Hum. Mol. Genet. *9*, 1487–1493.

Trinh, M.A., Kaphzan, H., Wek, R.C., Pierre, P., Cavener, D.R., and Klann, E. (2012). Brain-specific disruption of the eIF2α kinase PERK decreases ATF4 expression and impairs behavioral flexibility. Cell Reports *1*, 676–688.

Tsien, J.Z., Chen, D.F., Gerber, D., Tom, C., Mercer, E.H., Anderson, D.J., Mayford, M., Kandel, E.R., and Tonegawa, S. (1996). Subregion- and cell type-restricted gene knockout in mouse brain. Cell *87*, 1317–1326.

Vasudevan, S., and Steitz, J.A. (2007). AU-rich-element-mediated upregulation of translation by FXR1 and Argonaute 2. Cell *128*, 1105–1118.

Whitman, S.A., Cover, C., Yu, L., Nelson, D.L., Zarnescu, D.C., and Gregorio, C.C. (2011). Desmoplakin and talin2 are novel mRNA targets of fragile X-related protein-1 in cardiac muscle. Circ. Res. *109*, 262–271.

Yao, Y., Kelly, M.T., Sajikumar, S., Serrano, P., Tian, D., Bergold, P.J., Frey, J.U., and Sacktor, T.C. (2008). PKM zeta maintains late long-term potentiation by N-ethylmaleimide-sensitive factor/GluR2-dependent trafficking of postsynaptic AMPA receptors. J. Neurosci. *28*, 7820–7827.

Zhang, J., Hou, L., Klann, E., and Nelson, D.L. (2009). Altered hippocampal synaptic plasticity in the FMR1 gene family knockout mouse models. J. Neurophysiol. *101*, 2572–2580.